Interaction Notes

Note 448

May 1985

EMP-INDUCED, TIME-DOMAIN GRAZING SOLUTION FOR AN INFINITE WIRE OVER THE GROUND

Kenneth C. Chen
Electromagnetic Analysis Division
Sandia National Laboratories
Albuquerque, NM 87185

Abstract

The EMP-induced, time-domain current waveform is obtained for an infinite wire over the ground under grazing incidence. In contrast to previous results, the maximum grazing current is found to be slightly larger when the ground conductivity is higher. Also, the grazing angle for maximum current is found to be smaller when the ground conductivity is higher. For a ground conductivity of 10^{-2}S/m, the maximum current is approximately a factor of five larger than the typical value reported in the literature. A byproduct of this study is a simple formula of ground inductance for the transmission line mode.

Unlimited Release
SAND 85-0222

Acknowledgment

I thank K. M. Damrau for the numerical computations performed during the preparation of this report.

CONTENTS

FIGURES

INTRODUCTION AND SUMMARY

High altitude electromagnetic pulse (EMP) is an electromagnetic radiation of very short rise time, large amplitude, and brief duration that follows a nuclear explosion at 50 km or more above the earth's surface. The ground area that a single high-altitude EMP event can cover is very large; i.e., entire continents can be affected. The direction of incidence of the EMP radiation can vary from normal to grazing. The Defense Nuclear Agency, three services, and the Department of Energy expend resources in numerous research projects to understand the EMP coupling to electronics systems, power lines, and communication systems, and to design systems that would minimize harmful EMP effects.

This study is initiated by the need to determine the potential penetrating currents, induced by an EMP event, from overhead power lines and telephone lines through connectors to a C^3I ground station. The detailed physical layout of the overhead lines can affect the magnitude and the waveform of the induced line currents. Our objective here is to solve the simplest problem: an infinite wire over the ground under grazing incidence. The current calculated in this report is for a wire radius of 1 cm and a wire height of 10 m above the ground (Figure 1). A future report will address a long but finite horizontal wire over the ground under grazing incidence.

Although the problem of EMP coupling to overhead lines has been studied extensively in the past [1],[2], these calculations are not for grazing incidence but instead for a predetermined angle of incidence. A recent study [3] provides a new look at this old problem; however, the study is limited to the early-time solution and is not carried out for grazing incidence. The principal result reported here is that, in contrast to previous calculations [1] and [2], the maximum grazing current is found to be slightly larger as the ground conductivity increases. When a nominal incident EMP waveform of

$$E(t) = E_o e^{-t/\tau} \qquad (1)$$

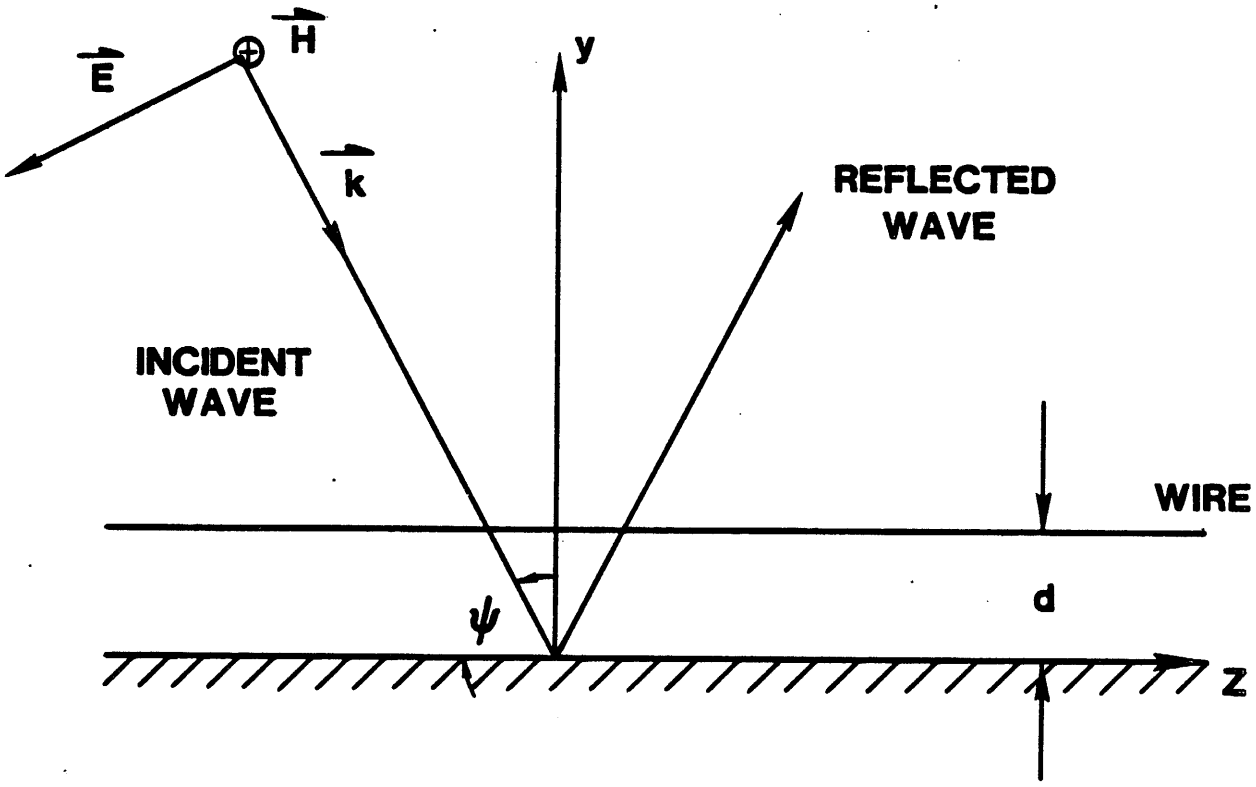

Figure 1. Configuration of a Wire Over the Ground Excited by an H-Polarized Incident Wave.

where

$$E_o = 50 \text{ kV/m}$$

$$\tau = 2.5 \times 10^{-7} \text{ sec} \qquad (2)$$

is assumed, the resulting induced line current is as follows. When the ground conductivity is 10^{-1} S/m the maximum grazing current of 9kA occurs at a grazing angle of 3° from the horizon. When the ground conductivity is 10^{-2} S/m, the maximum grazing current of 8.5 kA occurs at a grazing angle of 7°. When the ground conductivity is 10^{-3} S/m, the maximum current of 7 kA occurs at a grazing angle of 9° (Figures 8a through e). Comments on the current as a function of the grazing angle are given later.

This study is based on the well-known transmission line theory of Carson [4] and King et al. [5]. In a previous paper [6], the transmission line theory is used to solve the time-harmonic problem for a long horizontal wire over the ground with grazing incidence. The transmission line theory is used in this report to obtain the time-domain current for an infinite wire over the ground under grazing incidence of an EMP. This induced current is calculated in the following steps: First, the complicated formulas of the transmission line parameters are reduced to simple formulas whose deviation from the exact formulas is less than two percent. Second, the early-time waveform is obtained via a numerical inversion of the Laplace transform, a technique originally developed by Salzer [7]. Third, the Laplace transform of the induced current for a range in the transformed domain appropriate to the late-time solution is accurately approximated by a simple transform function, whose inverse transform is analytically available. Although the result is obtained by including only the transmission line mode, the major physical phenomenon of grazing comes from the beating of the transmission line mode and the incident wave. All other modes contribute much less to the induced wire current.

SIMPLE FORMULA OF GROUND INDUCTANCE

Ground Inductance in the Frequency Domain

As previously derived [4], [5], formulas for the transmission line wave number and characteristic impedance are given as ($e^{-i\omega t}$ time dependence)

$$k = (-ZY)^{1/2} \tag{3}$$

and

$$Z_c = (Z/Y)^{1/2} \tag{4}$$

with

$Y = -i\omega C$,

C = wire capacitance to the ground per meter = $\dfrac{2\pi\varepsilon_o}{\Omega}$,

$\Omega = \operatorname{arccosh}(d/a)$, a = wire radius

and d = wire height,

and

$Z = -i\omega L$,

$L = L_1 + L_2$

L_1 = wire inductance in air per meter = $\dfrac{\mu\Omega}{2\pi}$

L_2 = inductance in the ground per meter = $\dfrac{\mu\Delta}{2\pi}$.

Here Δ is given by

$$\Delta = 2\left\{\frac{1}{A^2} - \frac{K_1(A)}{A} + \frac{i\pi I_1(A)}{2A} - \frac{i\pi}{2A}\left[E_1(iA) - \frac{2}{\pi}\right]\right\} \tag{5}$$

with

$$\frac{i\pi}{2A}\left[E_1(iA) - \frac{2}{\pi}\right] = i\left[\frac{A}{3} + \frac{A^3}{45} + \frac{A^5}{1575} + \frac{A^7}{99225} + \cdots\right]. \tag{6}$$

I_1 and K_1 are the modified Bessel functions of the first and second kind, respectively, and the first order. E_1 is the Weber function of the first order, and finally, A is given by

$$A = 2k_4 d, \quad k_4 = \sqrt{\omega\mu(i\sigma_4 + \omega\varepsilon_0\varepsilon_{r4})} \quad . \tag{7}$$

Here k_4 is the wave number in the ground.

We use a previously reported method [8] for obtaining a uniform asymptotic formula for Δ. First, the small argument and large argument limits of Δ are sought, then a formula matching these two limiting cases is obtained. Thus, the small argument approximation of Δ is [6].

$$\Delta \sim -\ln\left(\frac{A}{2}\right) + i\frac{\pi}{2} = -\ln\left(-i\frac{A}{2}\right) \quad . \tag{8}$$

The large argument approximation of Δ is [6]

$$\Delta \sim \frac{2i}{A} \quad . \tag{9}$$

By inspection, a formula matching these two limiting cases is found to be

$$\Delta \sim \ln\left(\frac{1 - i\frac{A}{2}}{-i\frac{A}{2}}\right) \quad . \tag{10}$$

Figures 2 and 3 show the comparison of the exact evaluation of Δ given in [6] and the numerical value from using Equation 10 for Arg (A) = 45° and 0°, respectively. The two cases cover both the conducting and dielectric half space. The agreement is very good.

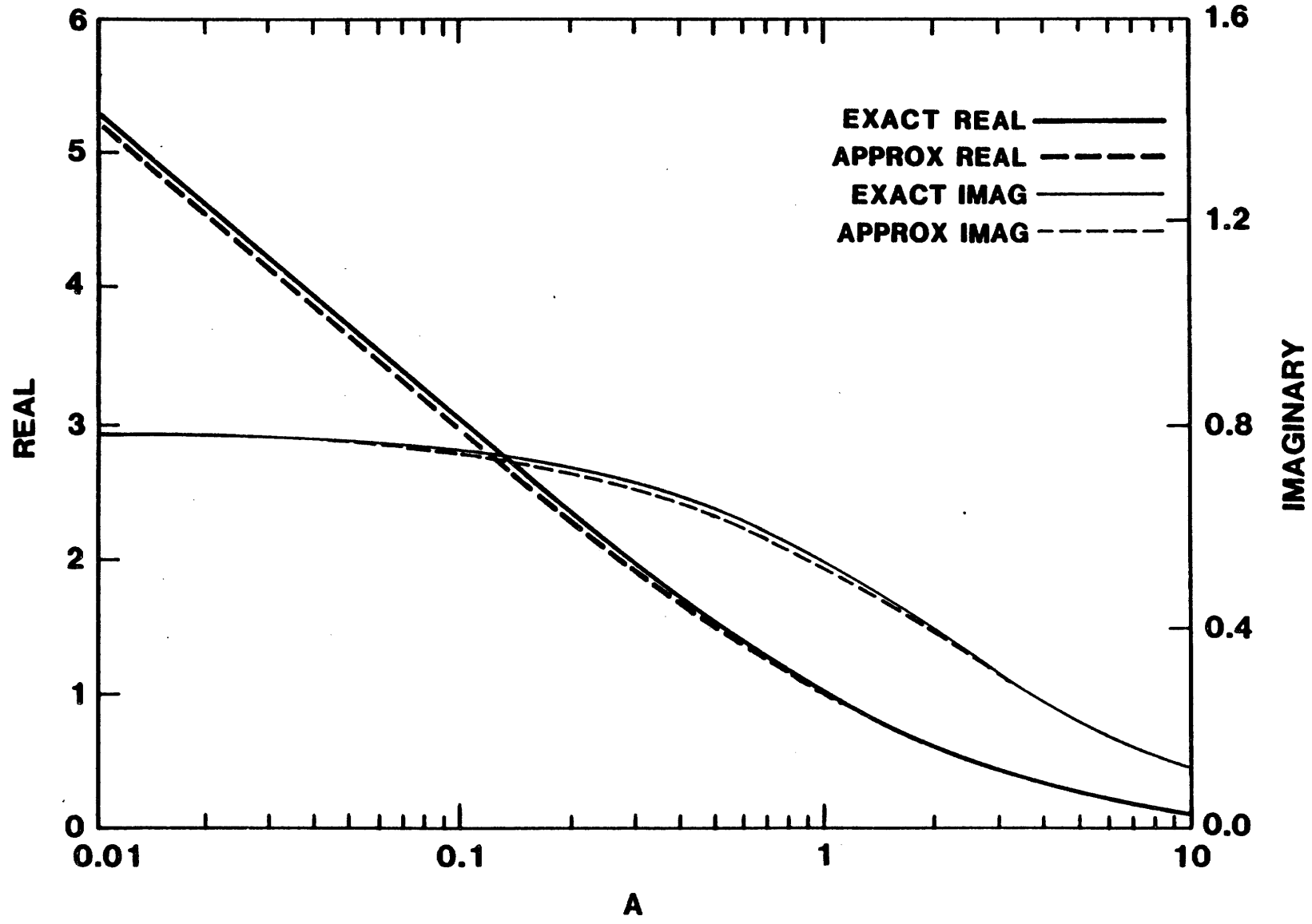

Figure 2. Comparison of the Exact Evaluation of Δ and an Approximate Formula (Equation 10) for $A = A\, e^{i\pi/4}$.

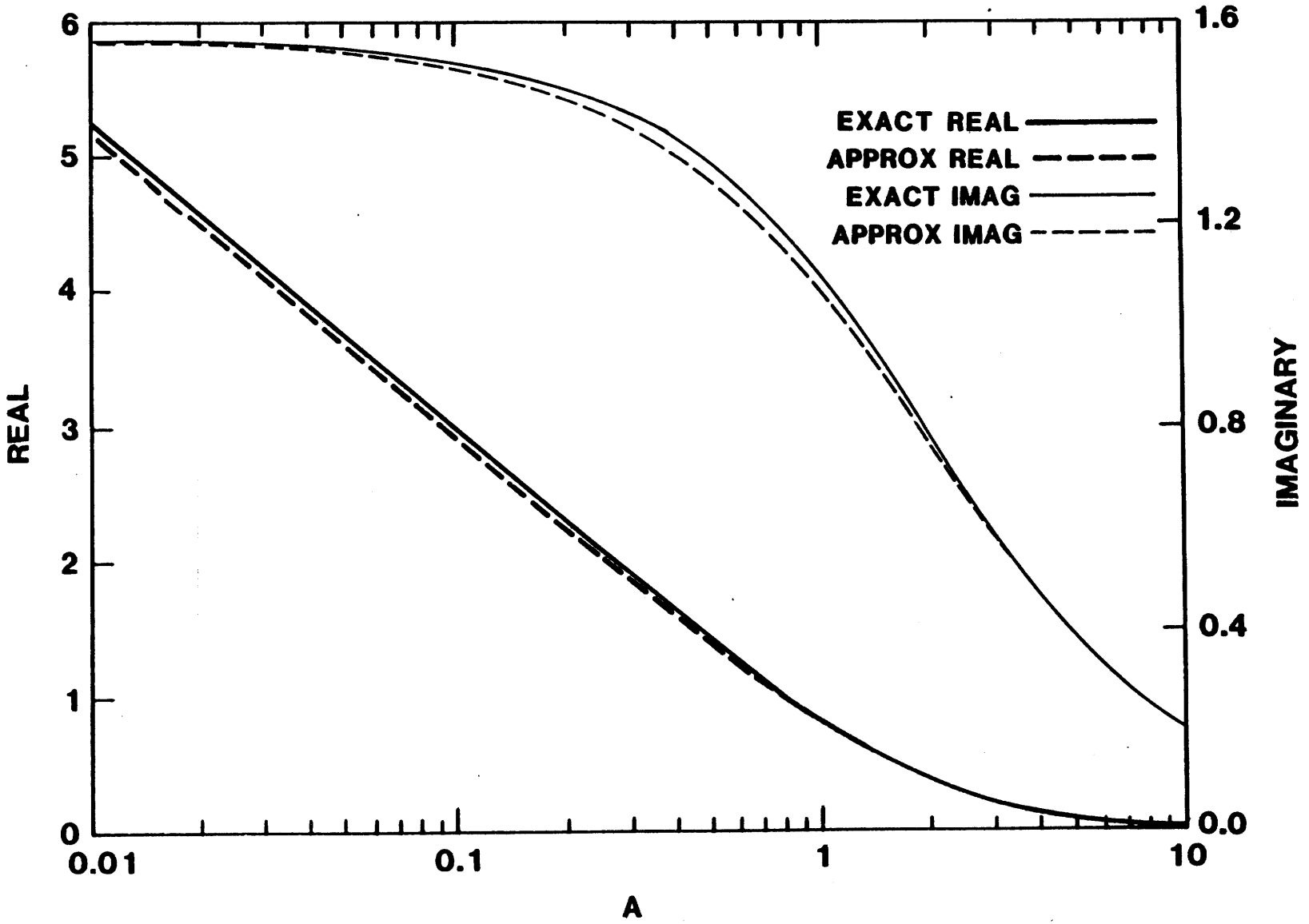

Figure 3. Comparison of the Exact Evaluation of Δ and Equation 10 for Real A.

Ground Inductance in the Laplace Transform Domain

The quantity of critical importance in the time-domain solution of this investigation is $\Delta(s)$, where $s = -i\omega$ (Appendix A). Two formulas for Δ are derived, one for numerical purposes, and the other for use in this paper.

First, to derive a formula for Δ_s convenient for the numerical purpose, we use Equation 12 in [6] and write it as follows:

$$\Delta(A) = \frac{2}{A^2} + 2i \int_0^1 (1 - x^2)^{1/2} \exp(-Ax)dx - \frac{2K_1(A)}{A}$$

$$= -\frac{2}{(-iA)^2} + 2 \int_0^1 (1 - x^2)^{1/2} \sin(-iAx)dx + \pi \frac{Y_1(-iA)}{(-iA)}$$

$$\Delta_s = -\frac{2}{A_s^2} + 2 \int_0^1 (1 - x^2)^{1/2} \sin A_s x \, dx + \frac{\pi Y_1(A_s)}{A_s} \quad . \tag{11}$$

where $$A_s = 2d\sqrt{s\mu(\sigma_4 + s\varepsilon_o\varepsilon_{r4})} \tag{12}$$

Notice the imaginary part vanishes because of an identity in a Bessel's function integral. A simple approximate formula for Δ_s can be obtained from Equation 10 as below.

$$\Delta_s \sim \ell n \left(\frac{1 + \frac{A_s}{2}}{\frac{A_s}{2}} \right) . \tag{13}$$

The comparison of Equations 11 and 13 is made in Figure 4 for Δ_s as a function A_s, and in Figure 5 for Δ_s as a function s for 12 decades, with d = 10m, a = 1 cm, $\sigma_4 = 10^{-2}$ S/m, and $\varepsilon_{r4} = 20$. The agreement is slightly better than the time-harmonic case.

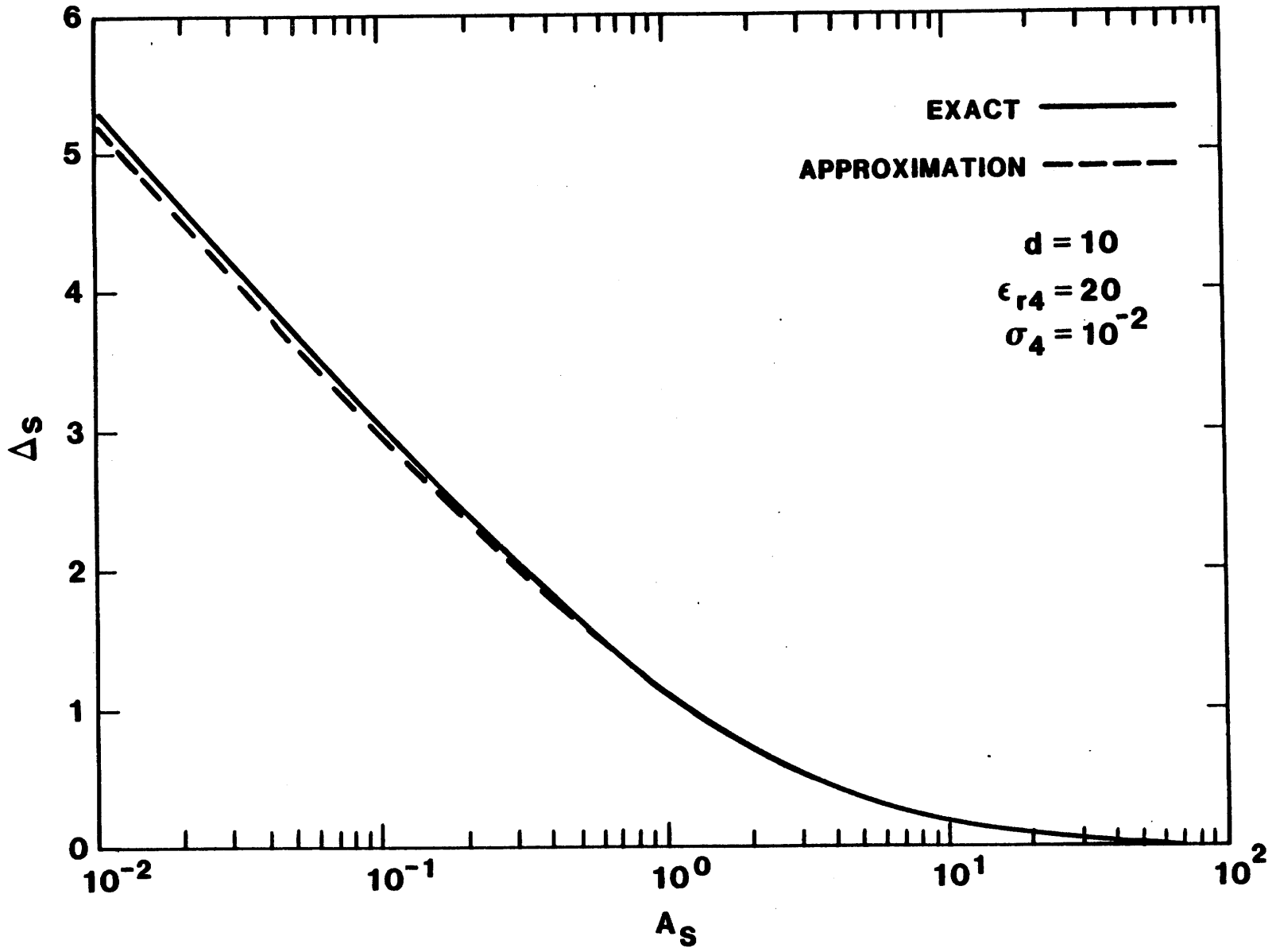

Figure 4. Comparison of the Exact Evaluation of Δ_s and Equation 13 as a Function of A_s.

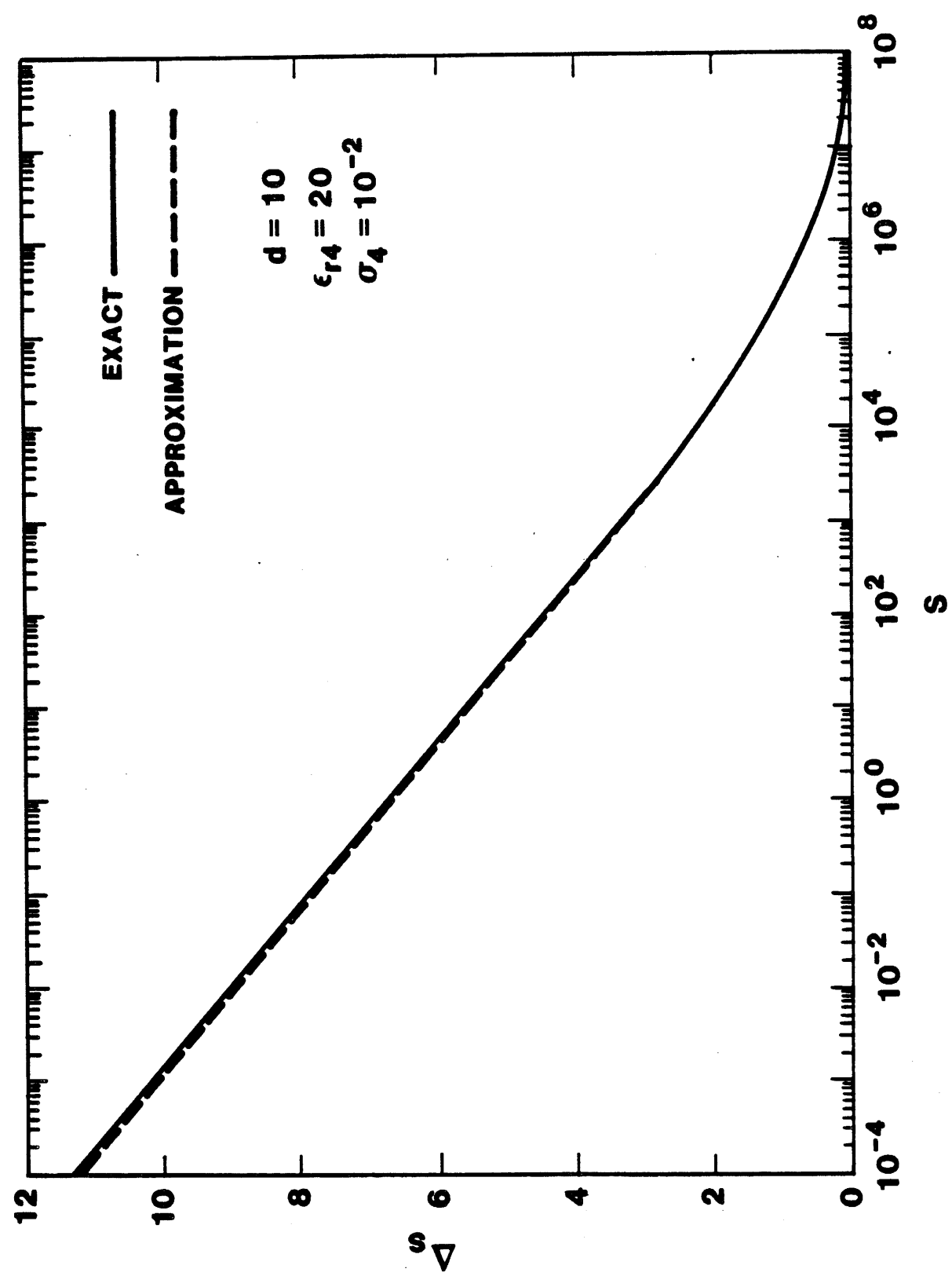

Figure 5. Comparison of the Exact Evaluation of Δ_s and Equation 13 for 12 Decades of s.

EARLY-TIME AND LATE-TIME BEHAVIORS OF THE GRAZING CURRENT

Grazing Current in the Laplace Transform Domain

For 1 V/m of incident time-harmonic field, the current on an infinite wire over the ground as shown in Figure 1 is given by (Appendix B)

$$I_\infty(\omega,z) = \frac{\sin\psi(1-R_h)}{2Z_c}\left[\frac{e^{ik_o z\cos\psi}}{i(k_o\cos\psi-k)} - \frac{e^{ik_o z\cos\psi}}{i(k_o\cos\psi+k)}\right], \tag{14}$$

where R_h is the reflection coefficient for the magnetic field parallel to the interface, i.e.

$$R_h = \frac{N^2\sin\psi - (N^2-\cos^2\psi)^{1/2}}{N^2\sin\psi + (N^2-\cos^2\psi)^{1/2}} \tag{15}$$

$$N = \frac{k_4}{k_o} . \tag{16}$$

This study is limited to the H-polarized case for grazing incidence, because the total electric field available for excitation is about a factor of five smaller for the E-polarized case than that for the H-polarized case.

In the Laplace transform domain, Equation 14 is

$$I_\infty(s,z) = \frac{c\,\sin\psi(1-R_{hs})}{2Z_o\zeta_{Ls}s}\left[\frac{e^{-sz(\cos\psi)/c}}{\zeta_{Ls}-\cos\psi} + \frac{e^{-sz(\cos\psi)/c}}{\zeta_{Ls}+\cos\psi}\right] \tag{17}$$

where

$$\zeta_{Ls} = \left(1 + \frac{\Delta_s}{\Omega}\right)^{1/2} \tag{18}$$

$$1 - R_{hs} = \frac{2(N_s^2 - \cos^2\psi)^{1/2}}{N_s^2 \sin\psi + (N_s^2 - \cos^2\psi)^{1/2}} \tag{19}$$

$$N_s^2 = \varepsilon_{r4} + \frac{\sigma_4}{s\varepsilon_o} \quad . \tag{20}$$

Because $\Omega \sim 6$, $\Delta_s < 2$ for $s > 10^3$, and $\zeta_{Ls} \sim 1$, for studying the grazing incidence, $\zeta_{Ls} \sim \cos\psi$. Therefore, the second term inside the parentheses of Equation 17 can be neglected. Thus, $I_\infty(s)$ is approximated by

$$I_\infty(s,z) = \frac{c \sin\psi(1-R_{hs})\, e^{-sz(\cos\psi)/c}}{2Z_o \zeta_{Ls} s\, (\zeta_{Ls} - \cos\psi)} \quad . \tag{21}$$

Since the exponent in Equation 21 only results in time delay in the time domain, we plot $I_\infty(s,0)$ in Figures 6a through e. The most important point to be noticed in these figures is in the range of s shown between points A and B on the curve. The curve can be approximated as a straight line on the log-log plot between these points; thus, $I_\infty(s,0)$ can be approximated as $s^{-\nu}$. For the case of $\sigma_4 = 10^{-1}$ S/m and $\psi = 3°$, given in Figure 6a, $\nu \sim 0.173$. For $\sigma_4 = 10^{-1.5}$ S/m and $\psi = 4°$ given in Figure 6b, $\nu \sim 0.256$. For $\sigma_4 = 10^{-2}$ S/m. and $\psi = 7°$ given in Figure 6c, $\nu \sim 0.33$. For $\sigma_4 = 10^{-2.5}$ S/m and $\psi = 9°$ given in Figure 6d, $\nu \sim 0.333$. For $\sigma_4 = 10^{-3}$ S/m and $\psi = 9°$, given in Figure 6e, $\nu \sim 0.42$. The grazing angle, ψ, is chosen such that the wire current is numerically determined to be the largest. Notice when ψ is chosen to be 30°, then $\nu \sim 0.5$. When this is the case, as is considered in [1] and [2], the denominator inside the parentheses in Equation 17 is a slowly varying function of s, and $\nu = 1/2$ is completely determined by $1 - R_{hs}$.

EMP Induced Grazing Current in the Laplace Transform Domain

The Laplace transform pair is given in Appendix A. Consider the problem of transient response due to an EMP with free-field time-domain waveform given as [1]:

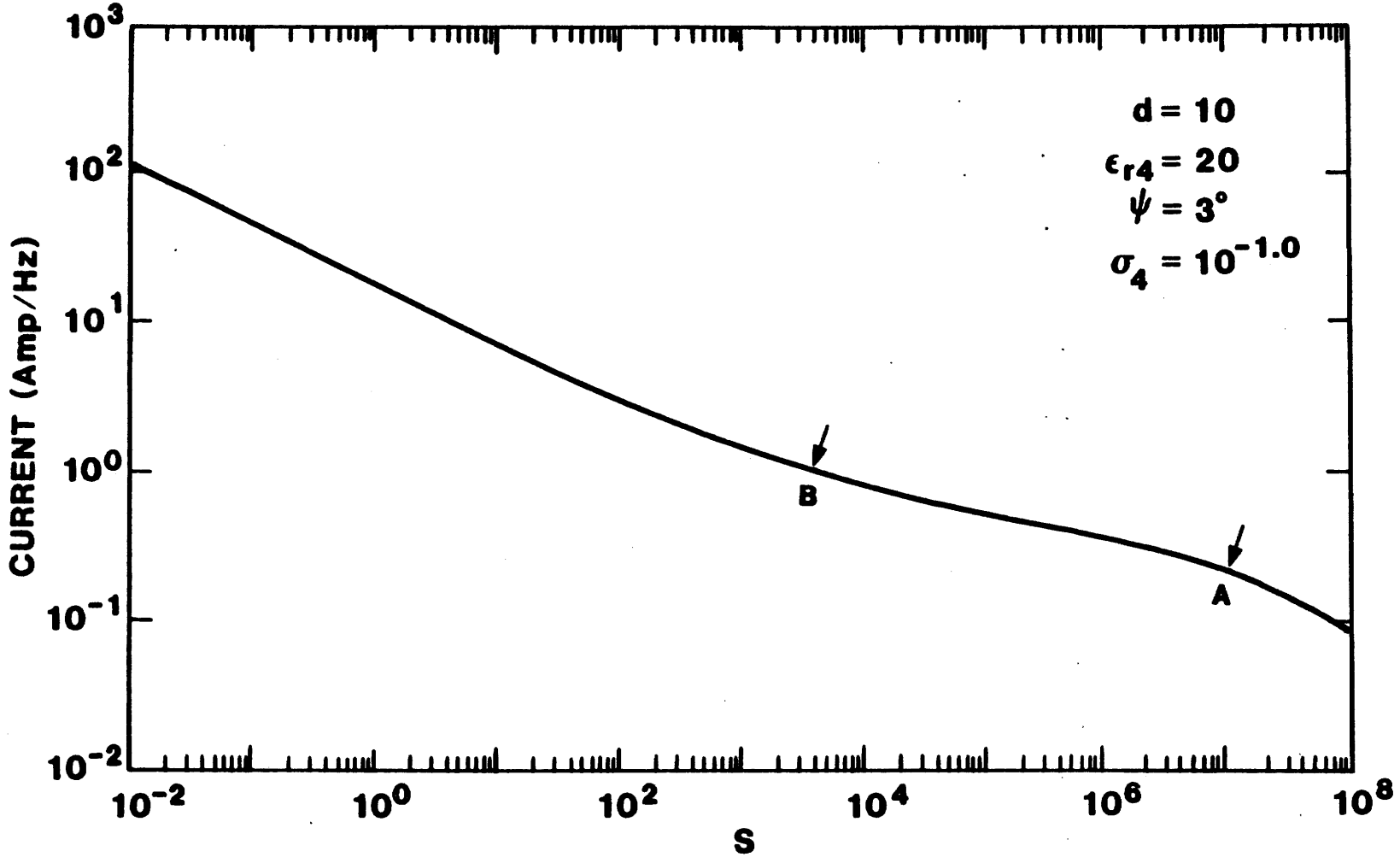

Figure 6a. Numerical Values of I_∞ (s,0) in a Log-Log Plot. (I_∞(s,0) can be Approximated by $s^{-\nu}$ for the Curve between A and B.)

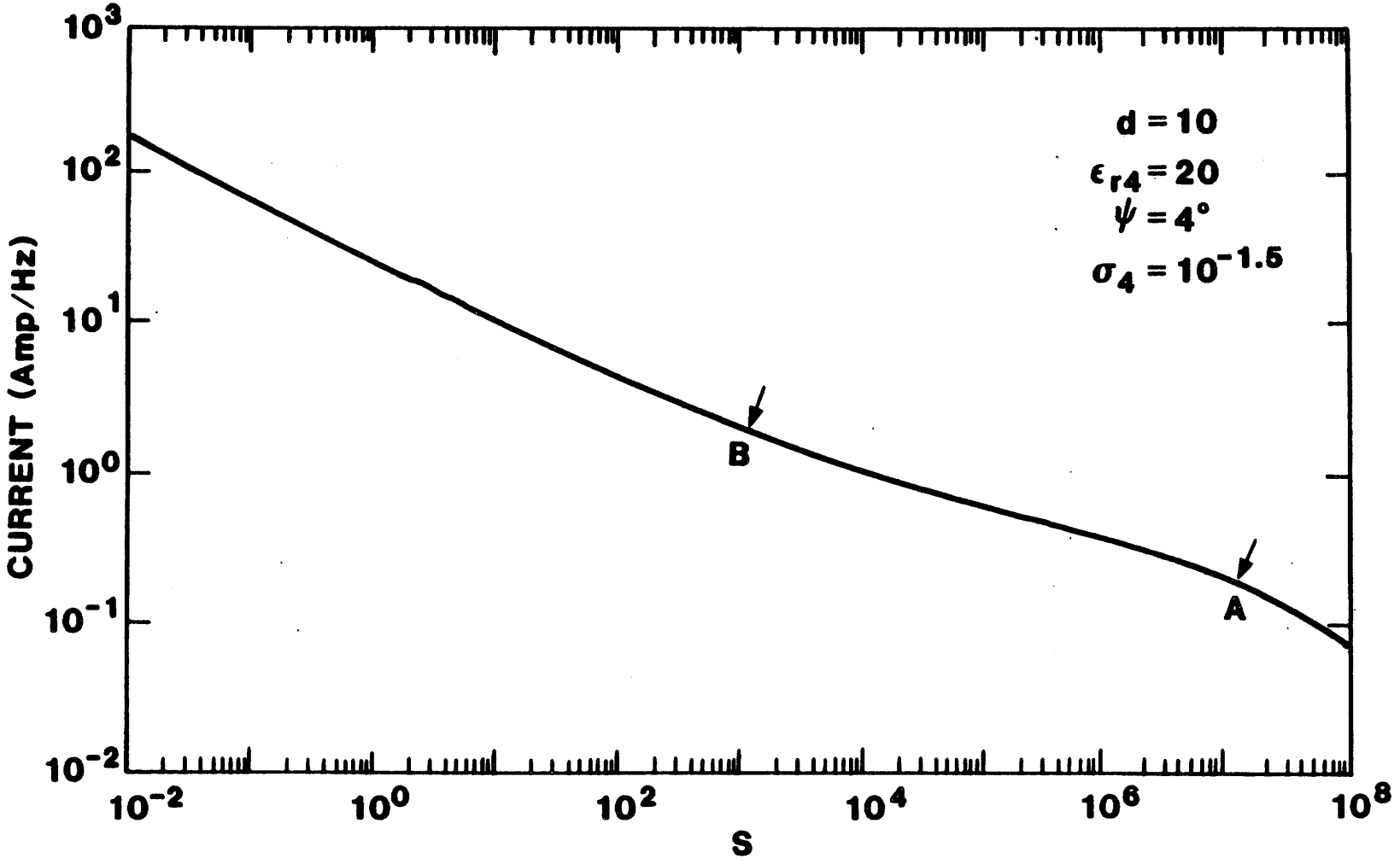

Figure 6b. Numerical Values of $I_\infty(s,0)$ in a Log-Log Plot. ($I_\infty(s,0)$ can be Approximated by $s^{-\nu}$ for the Curve between A and B.)

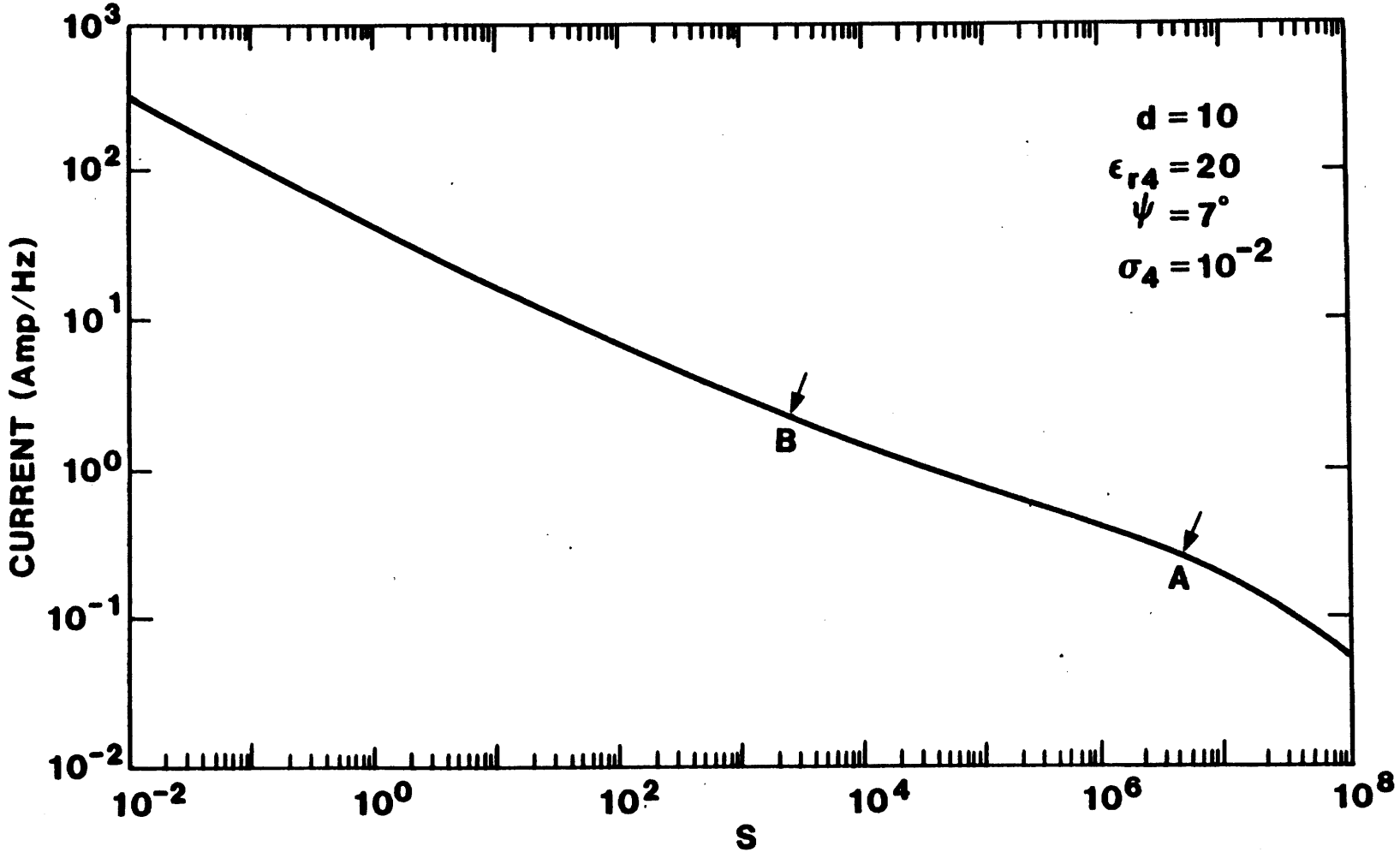

Figure 6c. Numerical Values of $I_\infty(s,0)$ in a Log-Log Plot. ($I_\infty(s,0)$ can be Approximated by $s^{-\nu}$ for the Curve between A and B.)

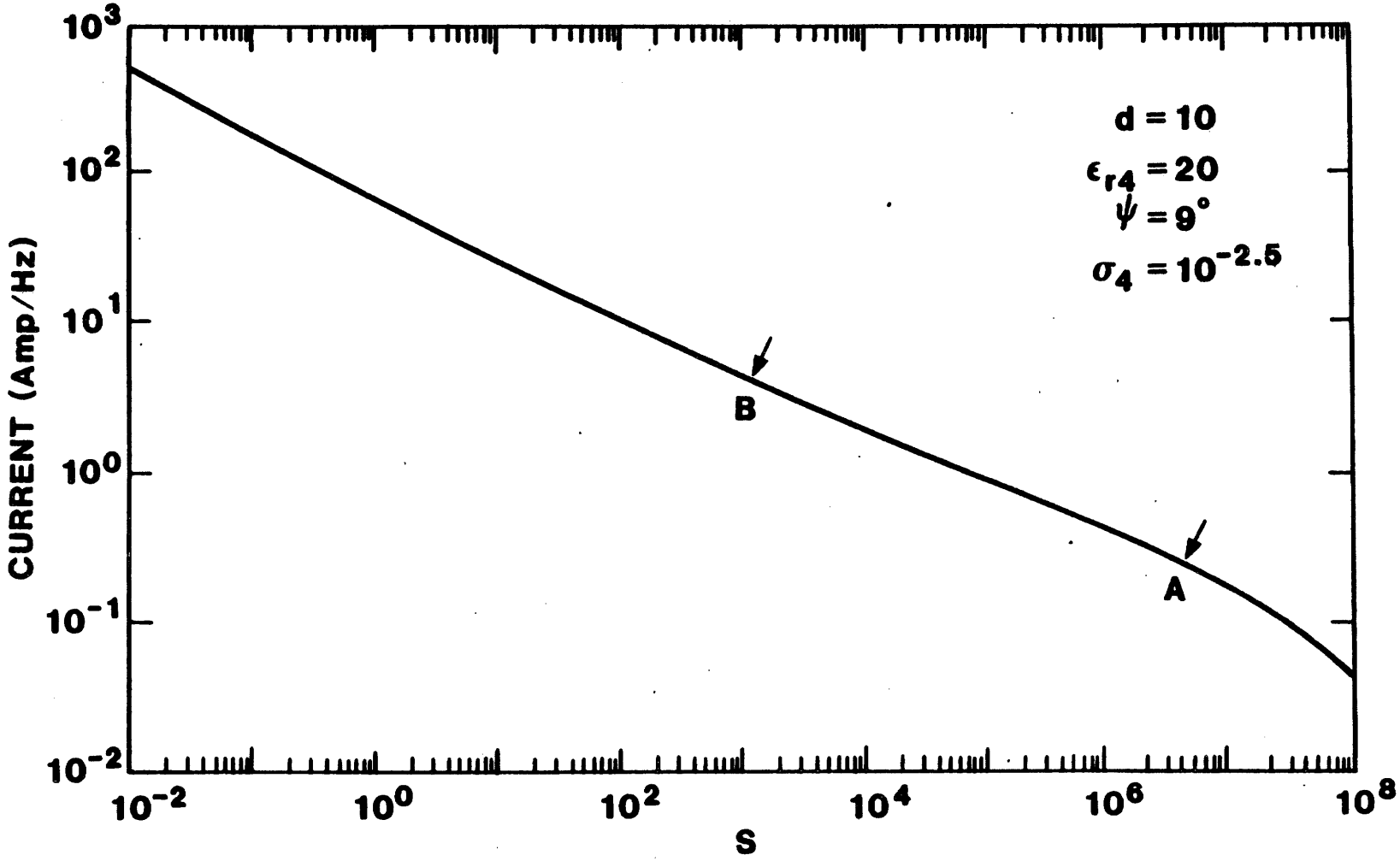

Figure 6d. Numerical Values of $I_\infty(s,0)$ in a Log-Log Plot. ($I_\infty(s,0)$ can be Approximated by $s^{-\nu}$ for the Curve between A and B.)

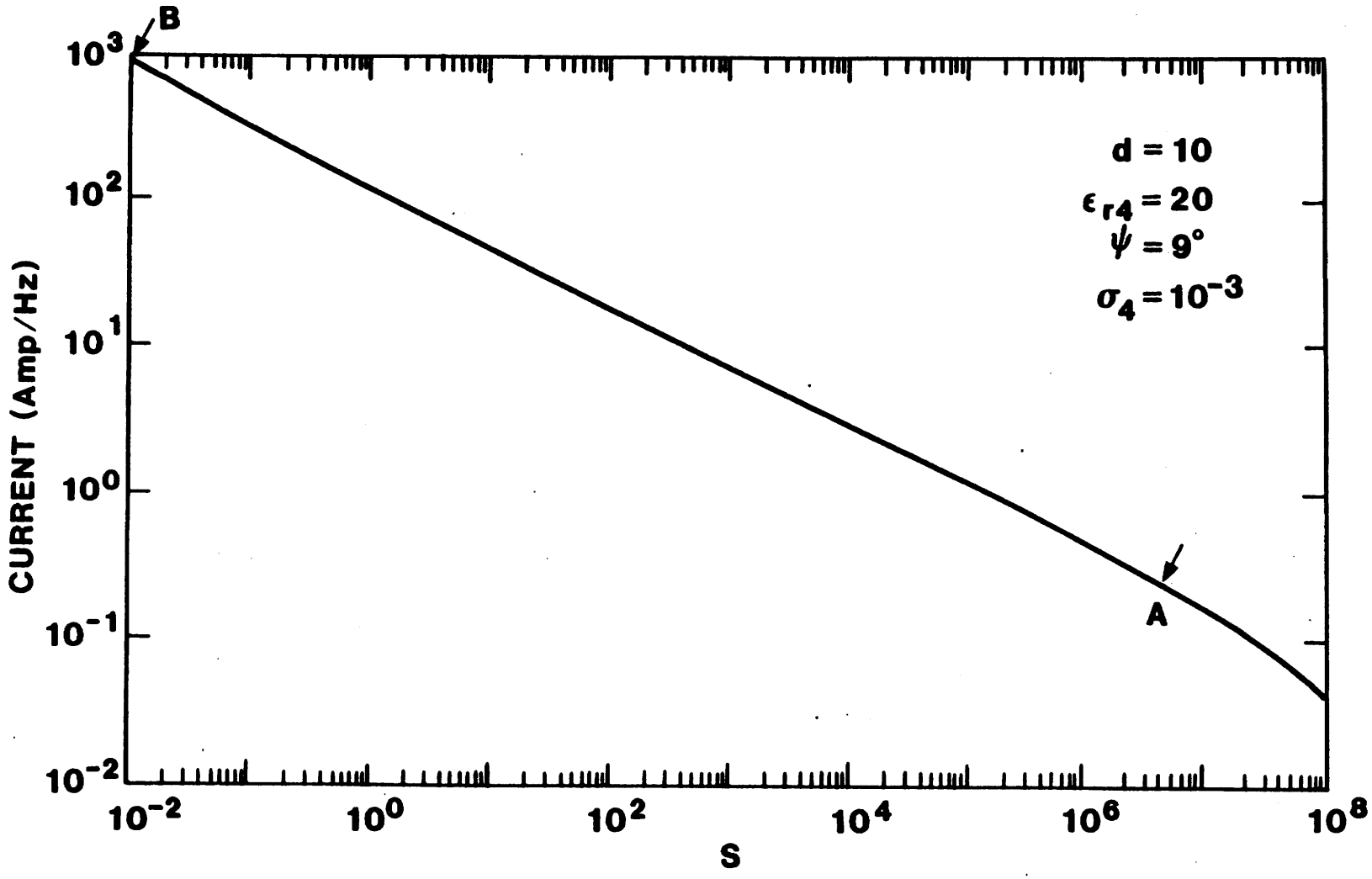

Figure 6e. Numerical Values of $I_\infty(s,0)$ in a Log-Log Plot. ($I_\infty(s,0)$ can be Approximated by $s^{-\nu}$ for the Curve between A and B.)

$$E(t) = E_o(e^{-t/t_f} - e^{-t/t_r}) - E_o e^{-t/t_f} \tag{22}$$

where

$$t_f = 2.5 \times 10^{-7} \text{ sec}$$
$$t_r = 2 \times 10^{-9} \text{ sec}$$
$$E_o = 5 \times 10^{4} \text{ V/m.}$$

The second term in Equation 22 gives rise to high frequency components which contribute negligibly to the grazing current. It can be ommitted. Thus, the Laplace transform of Equation 22 gives

$$E(s) = \frac{E_o}{s + t_f^{-1}} . \tag{23}$$

The time domain grazing current due to an EMP is given by

$$i_\infty(t,z) = i_\infty(\tau) = \frac{1}{2\pi i} \int_{-i\infty}^{i\infty} I_\infty(s)\, e^{s\tau} ds \tag{24}$$

where

$$I_\infty(s) = E_o I_\infty(s,0)\, (s + t_f^{-1})^{-1}$$
$$\tau = t - (z/c)\cos\psi$$
$$I_\infty(s,0) = I_\infty(s,z)\Big|_{z=0} . \tag{25}$$

Early-Time Behavior

To obtain the early-time behavior, we determine its transform as $s \to \infty$.

$$\lim_{s\to\infty} I_\infty(s) = \frac{E_o(\varepsilon_{r4} - \cos^2\psi)^{1/2}\, c \sin\psi}{\left[\varepsilon_{r4}\sin\psi + (\varepsilon_{r4} - \cos^2\psi)^{1/2}\right] Z_o(1-\cos\psi)s^2} \tag{26}$$

Then by Watson's theorem [9], [10]:

$$\lim_{\tau\to 0^+} \tau^{1-1/m}\, i_\infty(\tau) = \left[\Gamma\left(\frac{1}{m}\right)\right]^{-1} \lim_{s\to\infty} s^{1/m}\, I_\infty(s) \qquad (27)$$

we can let m be 1/2 and obtain

$$\lim_{\tau\to 0} i_\infty(\tau) = \frac{E_o(\varepsilon_{r4}-\cos^2\psi)^{1/2}\, c\sin\psi}{\left[\varepsilon_{r4}\sin\psi + (\varepsilon_{r4}-\cos^2\psi)\right]^{1/2} Z_o(1-\cos\psi)}\,\tau \,. \qquad (28)$$

This formula is used in the next section when we discuss the time domain grazing current.

Late-Time Behavior

It is possible also to apply Watson's theorem for $s\to 0$ and obtain a late-time approximation for $I_\infty(s)$. When this is done, $I_\infty(s) \sim s^{-1/2}$ and thus, $\lim_{\tau\to\infty} i_\infty(\tau) \sim \tau^{-1/2}$. However, for grazing incidence, as shown in Figures 6a through e, $I_\infty(s)$ does not quite approach $s^{-1/2}$ when $s = 10^{-2}$. When considering the inverse relationship between s and τ (the transform variables) τ has to be minutes before $i_\infty(\tau) \sim \tau^{-1/2}$.

When a few microseconds are considered as late time, as in the case of an EMP response, it is more appropriate to let

$$I_\infty(s,0) = As^{-\nu} \,. \qquad (29)$$

with values of ν for different physical parameters given at the end of the previous section. When we determine A from Equation 29 for the value $s = t_f^{-1}$, it follows

$$A = I_\infty(t_f^{-1},0)\, t_f^{-\nu} \,. \qquad (30)$$

Equations 25, 29 and 30 yield a late-time approximation for $I_\infty(s)$:

$$I_\infty(s) \sim E_o I_\infty(t_f^{-1},0)\, t_f^{-\nu}\, s^{-\nu}(s+t_f^{-1})^{-1} \,. \qquad (31)$$

On using an inverse transform formula [11], we have a late-time formula.

$$i_\infty(\tau) \sim E_o I_\infty(t_f^{-1},0) t_f^{-\nu} \frac{e^{-\tau/t_f}\,\tau^\nu}{\Gamma(\nu+1)} M(\nu;1+\nu;\tau/t_f) \qquad (32)$$

where

$M(\nu;1+\nu;x)$ = confluent hypergeometric function

$$= 1 + \frac{\nu}{1+\nu} x + \frac{\nu}{2+\nu}\frac{1}{2!} x^2 + \ldots + \frac{\nu}{n+\nu}\frac{1}{n!} x^n + \ldots \qquad (33)$$

and

$$\lim_{x\to\infty} M(\nu;1+\nu;x) = \nu e^x x^{-1} . \qquad (34)$$

Equation 32 is used in the next section. Notice the late-time limit in that equation is $\tau^{-1+\nu}$.

TIME DOMAIN GRAZING CURRENT

Numerical Inversion of Laplace Transforms

Numerical inversion of Laplace transforms is described in many textbooks. However, most techniques give good accuracy for the early time but not for the late time. We shall use a method originally due to Salzer [7] and described in [10] and [12]. Basically, polynomials for an optimum evaluation of the inverse Laplace transform integral have been found. These polynomials are expressed in terms of a ${}_2F_0$ hypergeometric series in [10]. The inverse Laplace transform is converted to a sum over their weights evaluated at the zero's of these polynomials. An explicit formula for the weights is given in [10]. Therefore, Equation 24 is written as

$$i_\infty(\tau) = \frac{1}{\tau}\frac{1}{2\pi i}\int_{-i\infty}^{i\infty} e^p\, I_\infty(\frac{p}{\tau})dp \qquad (35)$$

$$i_\infty(\tau) = \frac{1}{\tau}\frac{1}{2\pi i}\int_{-i\infty}^{i\infty} e^p\, p^{-2}\; p^2\, I_\infty(\frac{p}{\tau})\, dp \qquad (36)$$

$$= \frac{2}{\tau} \operatorname{Re} \sum_{k=1}^{n/2} p_k^2 \, I_\infty\left(\frac{p_k}{\tau}\right) A_k \qquad (37)$$

Equation 35 is obtained from Equation 24 by substituting $p = s\tau$. In Equation 36, p^{-2} has been factored out to have a correct behavior as $s \to \infty$ or $\tau \to 0$. P_k is the location of the zero and A_k is its corresponding weight. The conjugate property of the zeros has been used in Equation 37. We use the tables from [12] for N = 6, 8, and 12 for calculating the grazing current for $\sigma_4 = 10^{-1}$ S/m and $\psi = 3°$ (Figure 7), and the resulting numerical values are in good agreement. The tabulated values of P_k and A_k are listed in Appendix C. Finally, when $I_\infty(s)$ in Equation 37 includes a term arising from the second term inside the parentheses of Equation 17, no noticeable difference is observed in the numerical result.

Time Domain Grazing Current

We have presented two formulas, one for the very early time and the other for the late time, and a numerical method to obtain early and intermediate time. We now present the numerical value from the late-time formula and that from the numerical method in the same figure. The solid line in Figure 8a for $\sigma = 10^{-1}$ S/m and $\psi = 3°$ is from the numerical method and should be used until it crosses the dashed line, which is a late-time approximation. The figure shows the current only from 10^{-9} sec. To extend before that, one only needs to use Equation 28. Figures 8b, c, d, and e show the same information for $\sigma_4 = 10^{-1.5}$ S/m, $\psi = 4°$; $\sigma_4 = 10^{-2}$ S/m, $\psi = 7°$; $\sigma_4 = 10^{-2.5}$ S/m, $\psi = 9°$; $\sigma_4 = 10^{-3}$ S/m and $\psi = 9°$; respectively. We have also investigated the sensitivity of the grazing current to the angle ψ. When $\sigma_4 = 10^{-1}$ S/m, the peak current and the waveform remain about the same as ψ varies between 2.5° and 4.5°. When $\sigma_4 = 10^{-1.5}$ S/m, 10^{-2} S/m, $10^{-2.5}$ S/m, and 10^{-3} S/m, the peak current and the waveform are about identical when ψ varies between 3° and 6°, between 5° and 9°, between 7° and 11°, and between 8° and 13°, respectively. The variation in the peak current in these ranges of ψ is only about 5 percent.

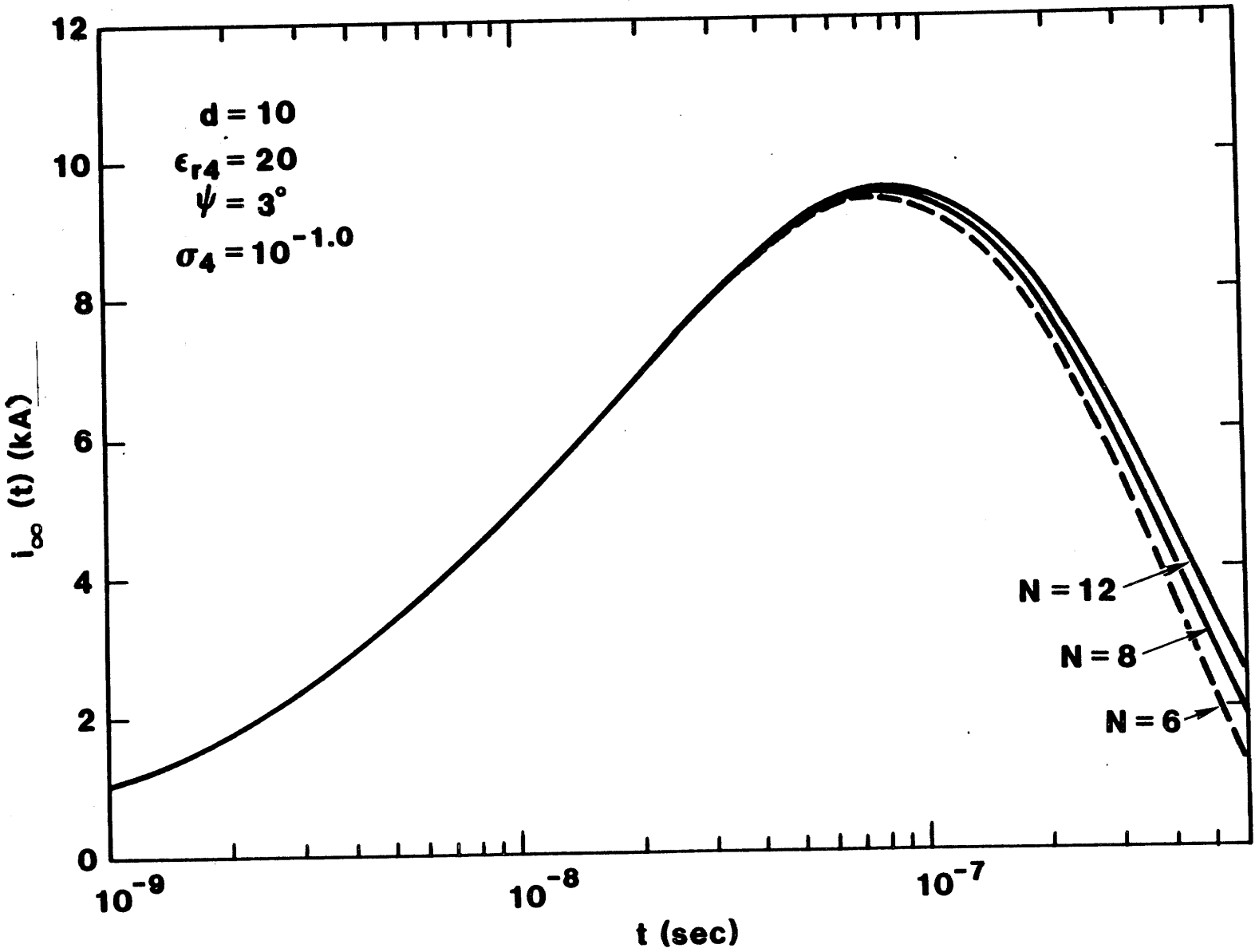

Figure 7. Comparison of the Numerical Inversion of Laplace Transform (Equation 37) with N = 6, 8, and 12.

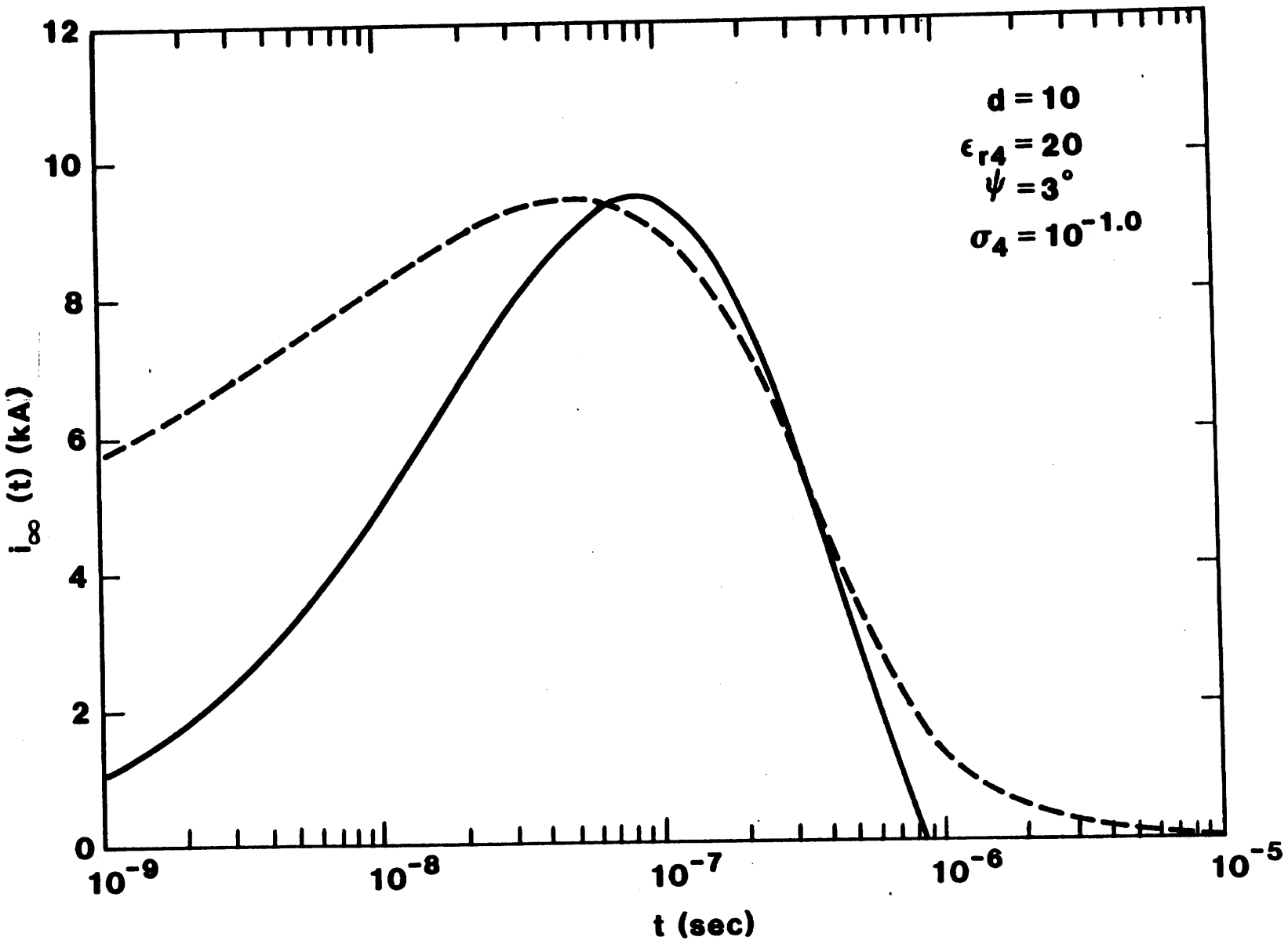

Figure 8a. The Solid Line is Obtained by the Numerical Inversion of Laplace Transform for N = 8. The Dashed Line is from Equation 32. The Waveform from t = 0 to 10^{-9} sec is given by Equation 28.

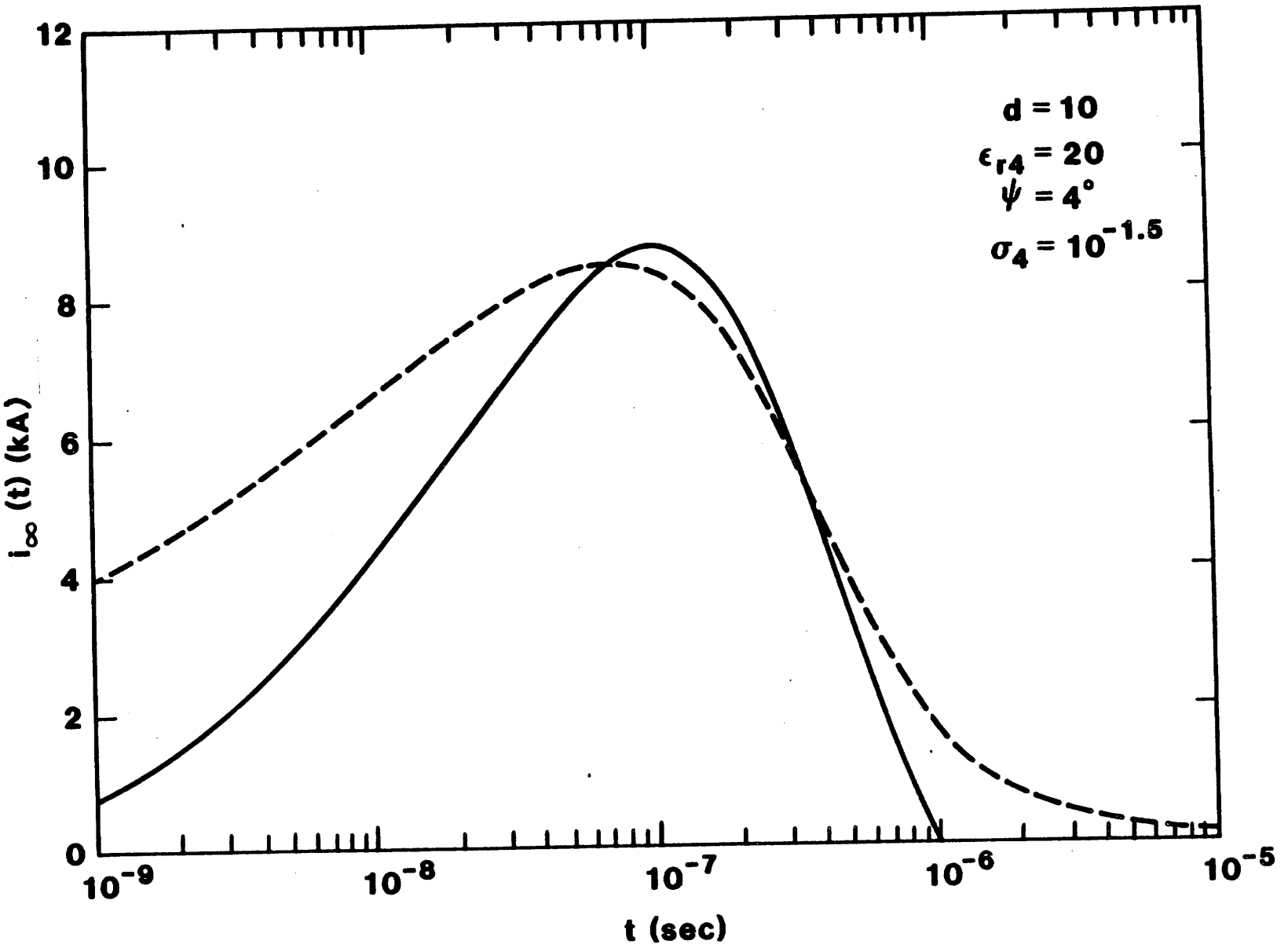

Figure 8b. The Solid Line is Obtained by the Numerical Inversion of Laplace Transform for N = 8. The Dashed Line is from Equation 32. The Waveform from t = 0 to 10^{-9} sec is given by Equation 28.

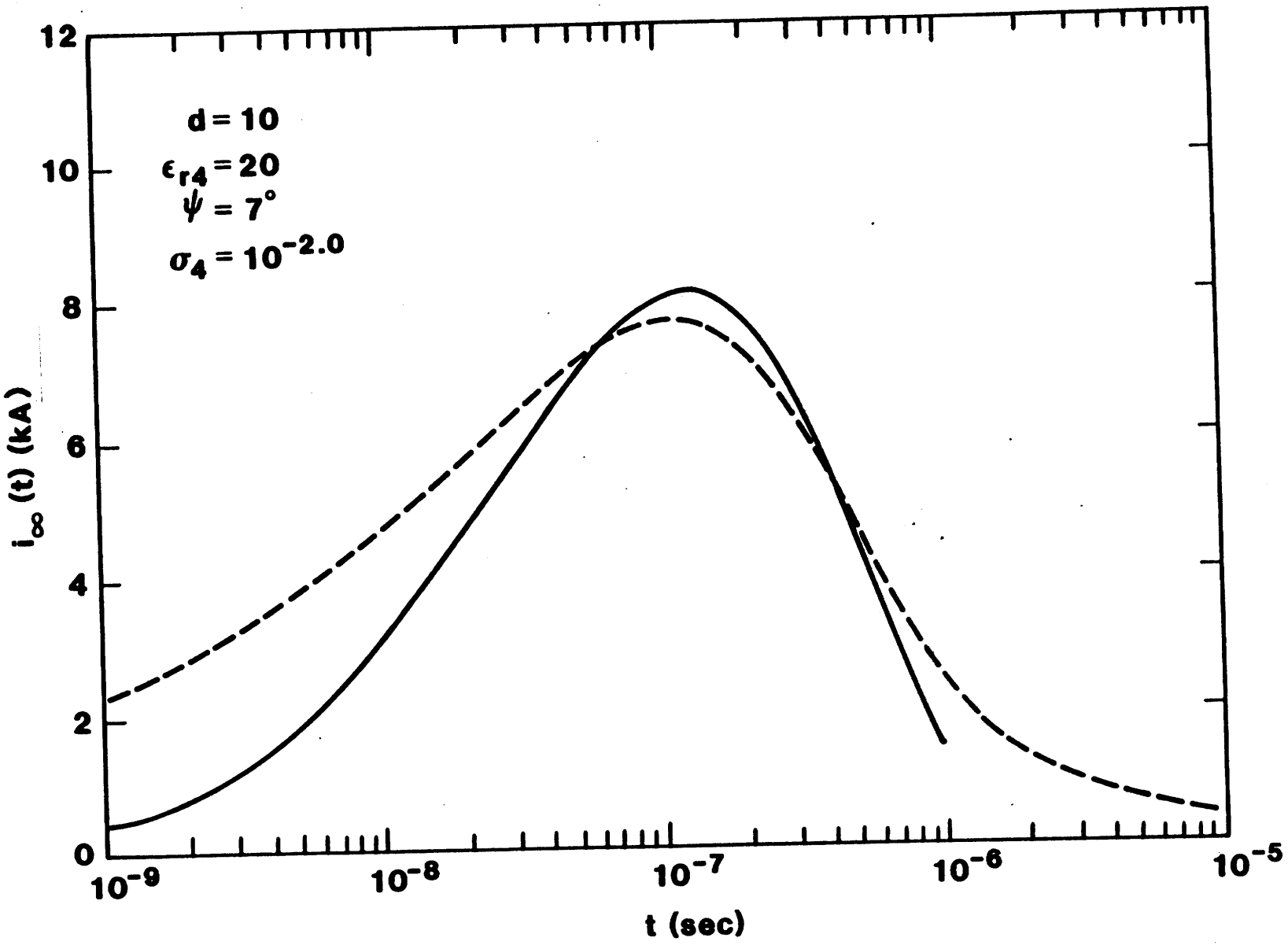

Figure 8c. The Solid Line is Obtained by the Numerical Inversion of Laplace Transform for N = 8. The Dashed Line is from Equation 32. The Waveform from t = 0 to 10^{-9} sec is given by Equation 28.

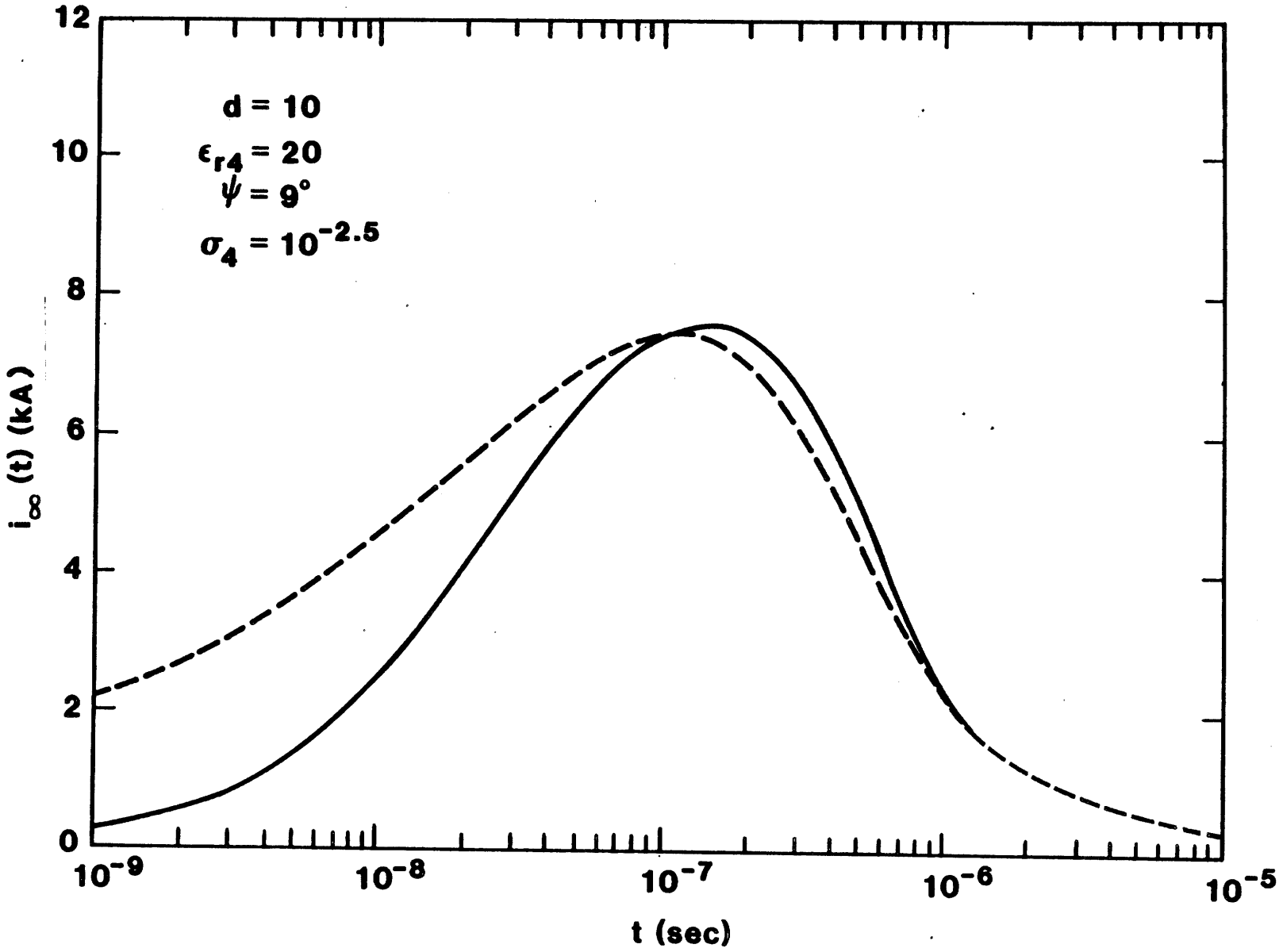

Figure 8d. The Solid Line is Obtained by the Numerical Inversion of Laplace Transform for N = 8. The Dashed Line is from Equation 32. The Waveform from t = 0 to 10^{-9} sec is given by Equation 28.

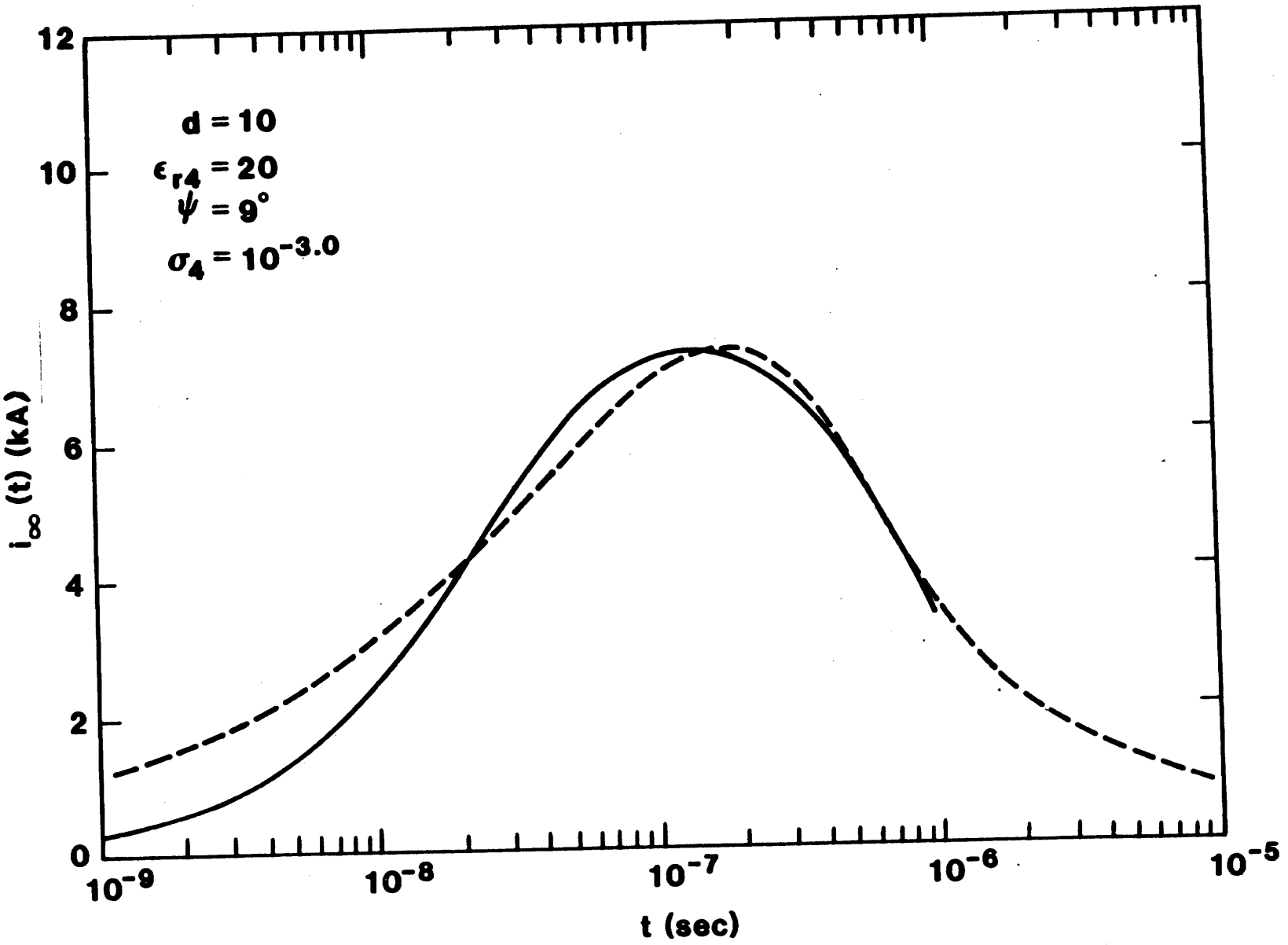

Figure 8e. The Solid Line is Obtained by the Numerical Inversion of Laplace Transform for N = 8. The Dashed Line is from Equation 32. The Waveform from t = 0 to 10^{-9} sec is given by Equation 28.

CONCLUSIONS

This report presents the calculated grazing current of an infinite horizontal wire over the ground. In contrast to the previous results, the maximum grazing current is found to be slightly higher when the ground conductivity increases. The grazing angle for maximum current is also found to be smaller when the ground conductivity is higher. We have presented results from a numerical method and two analytical formulas for the very early time and the late time.

APPENDIX A

Laplace and Fourier Transform Pairs

The convention used in this report is defined as follows:

$$\int_0^\infty e^{-st} f(t)dt = F(s) \tag{A1}$$

$$\frac{1}{2\pi i} \int_{-i\infty}^{i\infty} e^{ts} F(s)ds = f(t)u(t) \tag{A2}$$

for the Laplace transform pair. u(t) is the unit step function. Letting $s = -i\omega$ in Equation A1 and A2, we have

$$\int_{-\infty}^{\infty} e^{i\omega t} f(t)u(t)dt = F(-i\omega) \tag{A3}$$

$$\frac{i}{2\pi} \int_{-\infty}^{\infty} e^{-i\omega t} F(-i\omega)d\omega = f(t)u(t) \tag{A4}$$

for the Fourier transform pair. The theory concerning the property of these transform pairs is discussed in appropriate textbooks.

APPENDIX B

Time Harmonic Solution for a Horizontal Wire

Let K_V and K_I be Green's functions to the following transmission line equations:

$$\begin{cases} \dfrac{\partial K_V}{\partial z} + Z\, K_I = \delta(z-z') \\ \dfrac{\partial K_I}{\partial z} + Y\, K_V = 0 \end{cases} \tag{B1}$$

Then

$$K_I(z,z') = \frac{1}{2Z_c} \begin{cases} e^{ik(z-z')} & \text{for } z > z' \\ e^{ik(z'-z)} & \text{for } z < z' \end{cases}. \tag{B2}$$

where

Z_c and k are given by Equations 3 and 4.

For a 1 V/m of incident field, the electric field available for exciting the wire current is given by

$$E_z(z) = \sin\psi(1-R_h)\, e^{ik_o z\cos\psi} \tag{B3}$$

where R_h is given in Equation 19. Here the phase associated with the reflected wave is small and thus ignored.

The induced wire current can be shown easily to be

$$I(z) = \int_{-\infty}^{\infty} K_I(z,z')E_z(z')dz' = \text{Equation 14}\ . \tag{B4}$$

APPENDIX C

P_k and A_k for Numerical Inversion of Laplace Transforms

```
* N=6
C
C      DATA AK /( .319834709323091,  1.17903142140716),
C     >          (-3.40926161032703, -12.7197770038867),
C     >          ( 3.58942690100394,  36.2260472909385)/
C      DATA PK /( 5.03186449562164,  8.98534590730788),
C     >          ( 7.47141671265162,  5.25254462289425),
C     >          ( 8.49671879172672,  1.73501934646273)/
C
* N=8
C
C      DATA AK /( .273787695196975, -1.38993184986796),
C     >          ( 1.71575630183273,  27.6350460518111),
C     >          (-12.8627467739466, -144.255215387796),
C     >          ( 11.3732027769169,  310.173377206929)/
C      DATA PK /( 5.67796789779526,  12.7078225972097),
C     >          ( 8.73657843440480,  8.82888500094307),
C     >          ( 10.4096815812737,  5.23235030528505),
C     >          ( 11.1757720865261,  1.73522889070557)/
C
* N=12
C
       DATA AK /( 1.85725794270332, -.485839349727535),
      >          (-56.3909015285137,  70.9293584364054),
      >          ( 402.311652034329, -1059.09324671542),
      >          (-1188.68811805846,  6060.54780701406),
      >          ( 1668.17876227864, -17724.6940274801),
      >          (-826.768652668701,  29662.0417840153)/
       DATA PK /( 6.68604661560506,  20.2485936144816),
      >          ( 10.6594171817516,  16.1058137285140),
      >          ( 13.2220084999127,  12.3430699860744),
      >          ( 14.9311424807035,  8.74033918670913),
      >          ( 15.9945411992028,  5.21813307389159),
      >          ( 16.5068440228241,  1.73538714401953)/
```

REFERENCES

1. K. S. H. Lee, ed, EMP Interaction: Principles, Techniques, Reference Data, EMP Interaction 2-1 (Albuquerque, NM: AFWL, Kirtland AFB, December 1980).

2. E. F. Vance, Coupling to Shielded Cable (NY: John Wiley, 1978).

3. K. S. H. Lee, F. C. Yang, and N. Engheta, Interaction of High-Altitude Electromagnetic Pulse (HEMP) with Transmission and Distribution Lines: An Early-Time Consideration, Interaction Note 435 (Albuquerque, NM: Air Force Weapons Lab's Interaction Note Series).

4. J. R. Carson, "Wave Propagation in Overhead Wires with Ground Return," Bell System Tech Journal, Vol. 5, 1926, pp. 539-554.

5. R.W.P. King, T. T. Wu, and L. C. Shen, "The Horizontal-Wire Antenna Over a Conducting or Dielectric Half-Space: Current and Admittance," Radio Science, Vol. 9, July 1974, pp. 701-709.

6. K. C. Chen, "Time Harmonic Solutions for a Long Horizontal Wire Over the Ground with Grazing Incidence," Interaction Note 447 (Albuquerque, NM: Air Force Weapons Laboratory/NTAAB, October 1974).

7. H. E. Salzer, "Orthogonal Polynomials Arising in the Numerical Evaluation of Inverse Laplace Transforms," Journal of Mathematics and Computation, Vol. 9, 1955, pp. 164-177.

8. K. C. Chen. "Simple Formulas of Time-Domain and Time-Harmonic Fields for an Infinite Cylindrical Antenna,"(Paper submitted to IEEE Transactions on Antennas and Propagations).

9. F. W. J. Olver, Asymptotic and Special Functions (New York: Academic Press, 1974).

10. Y. L. Luke, The Special Functions and Their Approximations, Vol. II (New York: Academic Press, 1969).

11. I. S. Gradshteyn and I. M. Ryzik, Tables of Integrals, Series and Products (New York: Academic Press, 1980), p. 320.

12. V. I. Krylov and N. S. Skoblya, Handbook of Numerical Inversion of Laplace Transforms, (Translated from Russian by D. Louirsh, Israel Program for Scientific Translations, 1969).